# Transport Simulation of Helical Plasmas Using the TASK/TX Code

Masaki MIKI, Atsushi FUKUYAMA and Mitsuru HONDA[1)]

*Graduate School of Engineering, Kyoto University, Sakyo-ku, Kyoto 606-8501, Japan*

[1)] *Japan Atomic Energy Agency, 801-1 Mukoyama, Naka 311-0193, Japan*

(Received 21 December 2009 / Accepted 8 April 2010)

It is widely accepted that the radial electric field strongly affects plasma confinement through the transport process. We have analysed the time evolution of the radial electric field and the radial transport in plasmas in a helical magnetic configuration by extending the TASK/TX code [M. Honda and A. Fukuyama, J. Comput. Phys. **227**, 2808 (2008)]. TASK/TX is a one-dimensional dynamic transport code originally developed for axisymmetric plasmas. A set of flux-surface averaged fluid equations is solved simultaneously, rather than a set of diffusion equations based on the flux-gradient relations. TASK/TX consists of one-dimensional two fluids (electron and ion) equations, Maxwell's equations and diffusion equations of neutrals. To apply TASK/TX to helical plasmas, we have included two additional effects; helical neoclassical viscosity force and diffusion due to magnetic braiding. Plasma transport simulation is carried out mainly using the LHD parameters. We obtained negative radial electric field (ion root) with ion heating and positive radial electric field (electron root) with electron heating. Effects of magnetic braiding are also studied.



Keywords: helical plasma, radial transport, radial electric field, transport simulation

DOI: 10.1585/pfr.5.S2040

## 1. Introduction

In toroidal plasmas, the radial electric field $E_r$ strongly affects plasma confinement through the transport process. In helical plasmas, equations based on the ambipolar condition [1] have been widely used to determine the radial electric field. Some of the equations include an ambiguous electric diffusion coefficient $D_E$. In this paper, we present simulation results of the radial profile and the time evolution of radial electric field and radial transport in helical plasmas by extending the TASK/TX code [2]. The TASK/TX is a one-dimensional dynamic transport code, which can simulate time evolution of the plasma fluid quantities including $E_r$, by solving a set of fluid equations, rather than a set of diffusion equations based on the flux-gradient relations.

In section 2, we give a brief description of the TASK/TX and explain the specific helical terms added to the original TASK/TX. In section 3, after reviewing traditional ambipolar equations to determine $E_r$, the time evolution equation of $E_r$ derived from the equations of motion in TASK/TX is shown. The results of numerical simulations will be presented in section 4, and we conclude this paper in section 5.

## 2. Transport Models

### 2.1 TASK/TX code

The TASK/TX is the one-dimensional dynamic transport code originally developed for axisymmetric plasmas, which solves a set of flux-averaged two-fluid equations. TASK/TX consists of flux-averaged Maxwell's equations, two-fluid equations for electrons and bulk ions, as well as diffusion equations for three groups of neutrals. By solving these equations simultaneously, radial profiles of the radial electric field, density, temperature, plasma rotation and so on are obtained. In order to apply TASK/TX to helical plasmas, we have introduced additional terms briefly described in the following subsections.

### 2.2 Helical neoclassical transport

The magnitude of the magnetic field $B = |\boldsymbol{B}|$ in the helical configuration is expressed in an approximate form:

$$B(r,\theta,\phi) \approx B_0 \{1 - \epsilon_{\mathrm{T}} \cos\theta - \epsilon_{\mathrm{H}} \cos(l\theta - m\phi)\}.$$

Here, $\epsilon_{\mathrm{T}}$ and $\epsilon_{\mathrm{H}}$ are toroidal modulation and helical modulation of the magnetic field, $l$ and $m$ are the poloidal and toroidal mode numbers. The helical ripple results in neoclassical viscosity in toroidal and poloidal directions, which leads to enhanced neoclassical diffusion in the low collisional regime. The helical neoclassical viscosity force $F_{s\theta}^{\mathrm{HNC}}$ and $F_{s\phi}^{\mathrm{HNC}}$ are derived as follows for species s.

The position of a particle on a magnetic surface can be described by $\zeta = l\theta - m\phi$. If $\partial\zeta/\partial t = 0$ then the particle moves along the twisted magnetic surface, while in the case of $\partial\zeta/\partial t \neq 0$, the moving particle experiences the helical neoclassical viscosity force $\boldsymbol{F}_{\mathrm{s}}^{\mathrm{HNC}}$ perpendicular to the

*author's e-mail: miki_m@p-grp.nucleng.kyoto-u.ac.jp*

twist of the magnetic field. Poloidal and toroidal components of $\boldsymbol{F}_{\rm s}^{\rm HNC}$ can be written with the helical neoclassical viscosity $\nu_{\rm s}^{\rm HNC}$ as follow [1]:

$$\begin{aligned}\begin{pmatrix} F_{s\theta}^{\rm HNC} \\ F_{s\phi}^{\rm HNC} \end{pmatrix} &= -\begin{pmatrix} \alpha_\theta \\ -\alpha_\phi \end{pmatrix} \frac{m_{\rm s} n_{\rm s} \nu_{\rm s}^{\rm HNC} \dfrac{\partial \zeta}{\partial t}}{\sqrt{(l/r)^2 + (m/R)^2}} \\ &= -m_{\rm s} n_{\rm s} \nu_{\rm s}^{\rm HNC} \\ &\quad \times \begin{pmatrix} \alpha_\theta^2 & -\alpha_\theta \alpha_\phi \\ -\alpha_\theta \alpha_\phi & \alpha_\phi^2 \end{pmatrix} \begin{pmatrix} u_{s\theta} \\ u_{s\phi} \end{pmatrix}, \end{aligned} \tag{1}$$

where

$$\alpha_\theta = \frac{l/r}{\sqrt{(l/r)^2 + (m/R)^2}},\ \alpha_\phi = \frac{m/R}{\sqrt{(l/r)^2 + (m/R)^2}}.$$

Here we used

$$\frac{\partial \zeta}{\partial t} = l\frac{\partial \theta}{\partial t} - m\frac{\partial \phi}{\partial t} = l\frac{u_\theta}{r} - m\frac{u_\phi}{R}.$$

Assuming $1/\nu$ regime and collisional detrapping regime, the helical neoclassical viscosity $\nu_{\rm s}^{\rm HNC}$ can be written as follow [1, 3]:

$$\nu_{\rm s}^{\rm HNC} = \frac{v_{Ts}^2 \epsilon_{\rm H}^{3/2}}{R^2 \nu_{\rm s}} \frac{1}{3 + 1.67 \dfrac{\epsilon_{\rm T} \epsilon_{\rm H} \omega_E^2}{\nu_{\rm s}^2}}. \tag{2}$$

Here $\omega_E = E_r/Br$ is $\boldsymbol{E} \times \boldsymbol{B}$ drift frequency.

### 2.3 Diffusion due to magnetic braiding

In helical plasmas, destroyed magnetic surfaces due to magnetic perturbation appear near the plasma edge and enhance the radial transport. In order to apply TASK/TX to helical plasmas, we added the radial diffusion terms due to destroyed magnetic surfaces.

For weakly collisional plasmas, diffusivity due to the magnetic braiding can be expressed as follows [4]:

$$D_r \equiv \frac{\left\langle (\Delta r)^2 \right\rangle}{\tau} = \frac{\left\langle (\Delta r)^2 \right\rangle v_{Ts}}{\lambda} = D_{\rm m} v_{Ts}. \tag{3}$$

Here, $\lambda = \tau v_{Ts}$ is the distance along the magnetic field, which corresponds to mean free path, and $D_{\rm m}$ is the spacial diffusion coefficient. Eq. (3) shows that the diffusivity due to the destroyed magnetic field is assumed to be proportional to the thermal velocity $v_{Ts}$ of the species s. We used a fixed profile for $D_{\rm m}$ in the present calculation as

$$D_{\rm m}(\rho) = \begin{cases} D_{\rm m0} \dfrac{(\rho - \rho_{\rm min})^2 (\rho_{\rm max} - \rho)^2}{((\rho_{\rm max} - \rho_{\rm min})/2)^4} \\ \qquad (\rho_{\rm min} < \rho < \rho_{\rm max}), \\ 0 \qquad (\text{otherwise}), \end{cases} \tag{4}$$

where $\rho$ is the normalized minor radius and $\rho_{\rm min}$ and $\rho_{\rm max}$ are the lower and the upper bound of the braided region. Here the maximum value of $D_{\rm m}$ is given as $D_{\rm m0} = D_{\rm m}((\rho_{\rm max} - \rho_{\rm min})/2)$.

## 3. Governing Equation for the Radial Electric Field

In the previous literatures, two methods have been used to determine the radial electric field [1]. The first is called as the algebraic ambipolar relation, which is expressed using the radial ambipolar particle flux $\Gamma_{\rm as}$ for species s:

$$\varepsilon_0 \frac{\partial}{\partial t} \left\{ \left( 1 + \frac{c^2}{v_{\rm A}^2} \right) E_r \right\} = -\sum_{\rm s} e_{\rm s} \Gamma_{\rm as}.$$

This equation has a difficulty that $E_r$ can change discontinuously in the radial direction. This difficulty can be avoided by the formulation including derivatives of the electric field.

$$\begin{aligned}\varepsilon_0 \frac{\partial}{\partial t} \left\{ \left( 1 + \frac{c^2}{v_{\rm A}^2} \right) E_r \right\} &= -\sum_{\rm s} e_{\rm s} \Gamma_{\rm as} \\ &\quad + \frac{1}{V'(r)} \frac{\partial}{\partial r} \left[ V'(r) \left( \sum_{\rm s} \frac{e_{\rm s}}{e} D_E \right) \frac{\partial E_r}{\partial r} \right], \end{aligned}$$

where $D_E$ is the electric diffusion coefficient given in [1].

Corresponding equation can be derived from the equations of motion in TASK/TX. Keeping the Lorentz forces, the perpendicular viscosty force and the neoclassical viscosity force in the poloidal and toroidal equations of motion, we obtain

$$\begin{aligned}&\varepsilon_0 \frac{\partial}{\partial t} \left\{ \left( 1 + \frac{c^2}{v_{\rm A}^2} \right) E_r \right\} \\ &= -\sum_{\rm s} \frac{B_\phi}{B^2} \left\{ \frac{1}{r^2} \frac{\partial}{\partial r} \left[ r^3 m_{\rm s} n_{\rm s} \mu_{\rm s} \frac{\partial}{\partial r} \left( \frac{u_{s\theta}}{r} \right) \right] + F_{s\theta}^{\rm NC} + F_{s\theta}^{\rm HNC} \right\} \\ &+ \sum_{\rm s} \frac{B_\theta}{B^2} \left\{ \frac{1}{r} \frac{\partial}{\partial r} \left( r m_{\rm s} n_{\rm s} \mu_{\rm s} \frac{\partial u_{s\phi}}{\partial r} \right) + F_{s\phi}^{\rm HNC} \right\}. \end{aligned} \tag{5}$$

Here, $F_{s\theta}^{\rm NC}$ is the axisymmetric neoclassical viscosity force in poloidal direction, which is valid in banana-plateau regime, defined as [5];

$$F_{s\theta}^{\rm NC} = -\sqrt{\pi} q^2 n_{\rm s} m_{\rm s} \frac{v_{Ts}}{qR} \frac{\nu_{s\theta}^*}{1 + \nu_{s\theta}^*} u_{s\theta}\ ,\quad \nu_{s\theta}^* \equiv \frac{\nu_{\rm s} qR}{\epsilon_{\rm T}^{3/2} v_{Ts}}\ ,$$

$F_{s\theta}^{\rm HNC}$ and $F_{s\phi}^{\rm HNC}$ are poloidal and toroidal components of the helical neoclassical viscosity defined in Eqs. (1)-(2). Observing Eq. (5), we find that the balance of neoclassical viscosity forces corresponds to the traditional ambipolar relation.

Solving equations of motion directly, we can describe the time evolution of the radial electric field more consistently than conventional ambipolarity equations.

## 4. Numerical Simulation

In the following simulation, we adopted typical parameters of the Large Helical Device (LHD):

$$R = 3.7\,\text{m},\ a = 0.60\,\text{m},\ b = 0.65\,\text{m},$$
$$l = 2,\ m = 10,\ \epsilon_{\rm H} = \epsilon_{\rm h0}\rho^2,\quad \epsilon_{\rm h0} = 0.2.$$

Here, $l$ and $m$ are the poloidal and toroidal pitch number, $R$ is the major radius, $a$ and $b$ are the minor and wall radius. Initial conditions were set as follow:

$$
\begin{aligned}
&n_{e0}(\rho) = n_{e0}(0) + [n_{e0}(0) - n_{e0}(1)](1-\rho^3),\\
&n_{e0}(0) = 1.0\times10^{19}\,\mathrm{m}^{-3}\,,\quad n_{e0}(1) = 1.0\times10^{18}\,\mathrm{m}^{-3}\,,\\
&T_{s0}(\rho) = T_{s0}(0) + [T_{s0}(0) - T_{s0}(1)](1-\rho^2)^2,\\
&T_{s0}(0) = 0.30\,\mathrm{keV}\,,\quad T_{s0}(1) = 0.02\,\mathrm{keV}\,,\\
&q_0(\rho) = q_0(0) + [q_0(0) - q_0(1)](1-\rho^2),\\
&q_0(0) = 2.0\,,\quad q_0(1) = 1.0.
\end{aligned}
$$

For comparison of the effect of magnetic braiding, we also used parameters of a typical small helical device:

$$
\begin{aligned}
&R = 1.3\,\mathrm{m},\ a = 0.35\,\mathrm{m},\ b = 0.38\,\mathrm{m},\\
&l = 2,\ m = 5,\ \epsilon_H = \epsilon_{h0}\rho^2,\quad \epsilon_{h0} = 0.1,\\
&n_{e0}(0) = 4.0\times10^{19}\,\mathrm{m}^{-3}\,,\quad n_{e0}(1) = 5.0\times10^{18}\,\mathrm{m}^{-3}\,,\\
&T_{s0}(0) = 0.30\,\mathrm{keV}\,,\quad T_{s0}(1) = 0.02\,\mathrm{keV}\,,\\
&q_0(0) = 3.0\,,\quad q_0(1) = 2.0.
\end{aligned}
$$

For anomalous transport coefficients, particle diffusivity $D$, perpendicular viscosity $\mu_s$ and thermal diffusivity $\chi_s$, empirical fixed profiles are used in the present analysis:

$$
\begin{aligned}
&D(\rho) = D(0) + [D(1) - D(0)]\,\rho^3,\\
&D(0) = 0.1\,\mathrm{m}^2/\mathrm{s}\,,\quad D(1) = 0.3\,\mathrm{m}^2/\mathrm{s},\\
&\mu_s(\rho) = \mu_s(0) + [\mu_s(1) - \mu_s(0)]\,\rho^2,\\
&\mu_s(0) = 3\,\mathrm{m}^2/\mathrm{s}\,,\quad \mu_s(1) = 30\,\mathrm{m}^2/\mathrm{s},\\
&\chi_s(\rho) = \mu_s(\rho).
\end{aligned}
$$

## 4.1 Ion-root confinement with ion heating

First we examined the dependence of plasma fluid quantities on the ion heating power $P_i^{RF}$ in the case of $P_i^{RF} = 0.2\,\mathrm{MW}$, $0.4\,\mathrm{MW}$, $0.6\,\mathrm{MW}$. Figure 1 shows the radial profiles of (a) radial electric field $E_r$, (b) electron density $n_e$, (c) safety factor $q$, (d) electron temperature $T_e$, (e-f) electron plasma rotation $u_{e\theta}$ and $u_{e\phi}$, (g) ion temperature $T_i$, (h-i) ion plasma rotation $u_{i\theta}$ and $u_{i\phi}$ at $t = 0.1$ s.

Negative $E_r$ is formed in all radial region, whose magnitude $|E_r|$ is almost proportional to the heating power. The electron density $n_e$ became lower as the heating power became stronger. In all cases, the density has decreased linearly as time advances.

## 4.2 Electron-root confinement with electron heating

Next we examined the dependence of radial profiles on the electron heating power $P_e^{RF}$ in the case of $P_e^{RF} = 0.2\,\mathrm{MW}$, $0.4\,\mathrm{MW}$, $0.6\,\mathrm{MW}$. Figure 2 (a-i) shows the radial profiles of $E_r$, $n_e$, $q$, $T_s$, $u_{s\theta}$ and $u_{s\phi}$ at $t = 0.5$ s as same as Fig. 1.

Contrast to the case of ion heating, positive $E_r$ peaking at $\rho \approx 0.1$ is observed in the case of higher electron heating power. The peak value of $E_r$ becomes larger as the heating power increases. Particle confinement becomes better with higher heating power. A hollow density profile where the density gradient becomes positive is observed at $\rho \lesssim 0.2$.

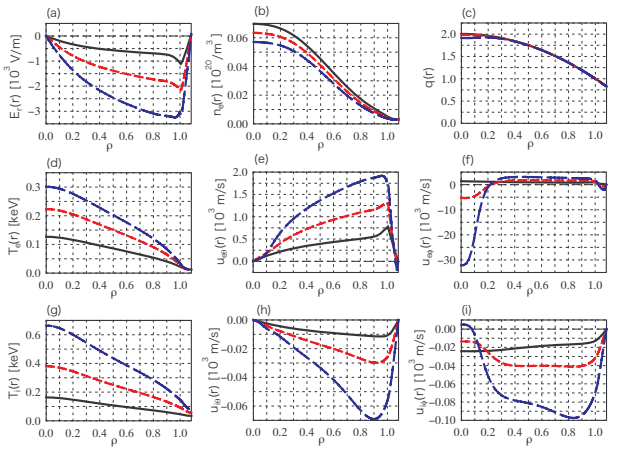


Fig. 1 Radial profiles for $P_i^{RF} = 0.2\,\mathrm{MW}$ (black), $0.4\,\mathrm{MW}$ (red) and $0.6\,\mathrm{MW}$ (blue).

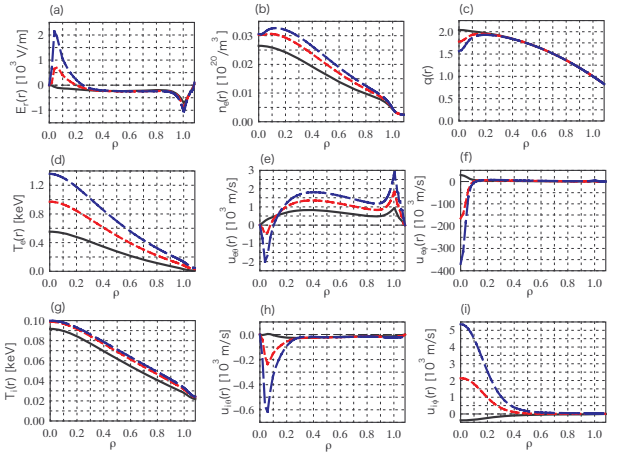


Fig. 2 Radial profiles for $P_e^{RF} = 0.2\,\mathrm{MW}$ (black), $0.4\,\mathrm{MW}$ (red) and $0.6\,\mathrm{MW}$ (blue).

We have also examined the time evolution of the radial electric field $E_r$ in the case with $P_e^{RF} = 0.4\,\mathrm{MW}$. Figure 3 shows the time evolution of (a) $E_r$ profile, (b) temperatures on magnetic axis $T_s(0)$ and averaged temperatures $\langle T_s\rangle$, (c) density on magnetic axis $n_e(0)$ and averaged density $\langle n_e\rangle$.

At the beginning of heating $E_r$ is negative in all region but the transition to $E_r > 0$ occurs near $\rho \approx 0.1$. We observed the same behavior in the case of $P_e^{RF} = 0.2\,\mathrm{MW}$ and $0.6\,\mathrm{MW}$, but the time of transition was earlier in the case of higher heating power and vice versa.

## 4.3 Effect of magnetic braiding

First we analysed the effects of destroyed magnetic surfaces in a typical small helical plasma. The radial profile of the magnetic diffusivity $D_m(\rho)$ is defined as Eq. (4). The lower and the upper bound of the braided region are set to $\rho_{min} = 0.85$ and $\rho_{max} = 1.02$, respectively, and the maximum value of $D_m(\rho)$ is $D_{m0} = 1.0\times10^{-8}$. The heat-

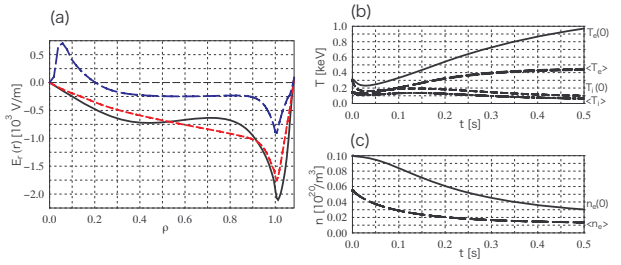


Fig. 3 Time evolution of the radial electric field. (a): Radial profiles of $E_r$ at $t = 0.10$ s (black), 0.30 s (red), 0.50 s (blue). (b): Time evolution of $T_s(0)$ and $\langle T_s \rangle$. (c): Time evolution of $n_e(0)$ and $\langle n_e \rangle$.

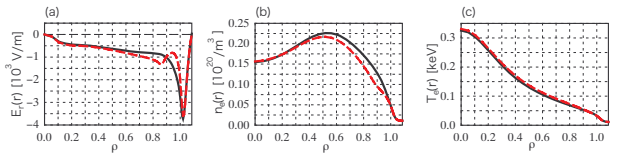


Fig. 4 Effect of magnetic braiding on (a) $E_r$, (b) $n_e$, and (c) $T_e$ of a typical helical plasma. The case without magnetic braiding (black) and the case with magnetic braiding (red).

ing power is $P_e^{RF} = 0.036$ MW. Figure 4 shows the radial profiles of (a) $E_r$, (b) $n_e$ and (c) $T_e$ at $t = 0.15$ s.

Sharp increase in $E_r$ is observed near the ergodic region. This can be understood as follow. It is clear from eq. (4) that in the ergodic region electrons diffuse more quickly than ions since $v_{Te} \gg v_{Ti}$, which results in the increase of $E_r$. Although the density slightly decreases inside the ergodic region, the temperature profiles are not affected. The difference may be explained by large heat transport mainly driven by the anomalous transport.

We also examined the effects of destroyed magnetic surfaces using the LHD parameters. The profile of $D_m(\rho)$ was set as same as in the previous calculation. The heating power is $P_e^{RF} = 0.2$ MW. Figure 5 shows the radial profile of (a) $E_r$, (b) $n_e$ and (c) $T_e$ at $t = 0.5$ s.

For LHD plasmas, remarkably large positive $E_r$ appeared in the ergodic region, while density and temperature profiles were not affected. The reason why the results which differ from the case of typical small helical plasma

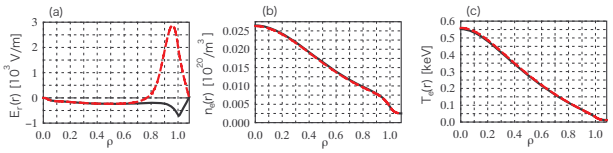


Fig. 5 Effect of magnetic braiding on (a) $E_r$, (b) $n_e$, and (c) $T_e$ in LHD plasma. The case without magnetic braiding (black) and the case with magnetic braiding (red).

were obtained are not clear and left for our future work.

## 5. Conclusion

In this study, we simulated the radial transport and the time evolution of the radial electric field in helical plasmas by extending the TASK/TX code. By changing the ion and electron heating power, the ion root and the electron root transport were obtained. In the case of the ion heating, only the ion root was observed. In the case of the electron heating, electron root has appeared near the magnetic axis. Effect of magnetic braiding was also studied for typical small helical plasmas and LHD plasmas.

A future work includes : 1) Comparison of the radial electric field which is obtained from TASK/TX and the usual ambipolar relation. 2) Study of parameters dependence of the existence and performance of electron root (anomalous transport model, density *et al.*) 3) Theory-based model for turbulence transport, such as current-diffusive interchange mode (CDIM) model instead of the fixed spacial profile.

## Acknowledgements

This work is supported by Grant-in-Aid for Scientific Research (S) (20226017) from JSPS, Japan.

[1] D. E. Hastings, W. A. Houlberg and K. C. Shaing, Nucl. Fusion **25**, 445 (1985).
[2] M. Honda and A. Fukuyama, J. Comput. Phys. **227**, 2808 (2008).
[3] D. E. Hastings, Phys. Fluids **28**, 334 (1985).
[4] A. B. Rechester and M. N. Rosenbluth, Phys. Rev. Lett. **40**, 38 (1978).
[5] S. P. Hirshman and D. J. Sigmar, Nucl. Fusion **21**, 1079 (1981).